CrossMark

Effects of temperature and frequency on the dielectric properties of AgPO$_3$ glass

A. Shaheen[1] · M. Maghrabi[1] · F. Salman[2] · Z. Khattari[1] (ID)

Abstract

The dielectric behavior of AgPO$_3$ glass network was studied at different temperatures and in the frequency range between 50 and 10^6 Hz using impedance spectroscopy technique. The glassy network was prepared by melting NH$_4$H$_2$PO$_4$ and AgNO$_3$ in the powder form using the mole ratio technique. The measured ac-conductivity shows two distinct regions. Over the whole temperature range, the conductivity is fairly constant at low frequency and a power law dispersive behavior was observed at higher frequency (i.e., $f > 10^4$ Hz). The power law exponent (s) was very close to unity while the crossover frequency (ω_p) was observed to increase with increasing temperature. The activation energy extracted from the Arrhenius linear plot of the dc-conductivity (σ_{dc}) was found to be E_a=0.47 eV.

1 Introduction

Continuing improvement of a large-scale multi-component material that transmits both electrical and light signals is an emerging field of extensive research [1–5]. In particular, phosphate-based glasses have received attention due to their high mechanical stability, chemical durability and high glass transition and crystallization temperatures [5, 6]. Several variants of glass-based phosphate pseudo-binary mixtures such as xAgI-$(1 − x)$AgPO$_3$ [7], xNaI-$(1 − x)$AgPO$_3$ [8] or when doped with other chemical groups such as WO$_3$ [5], RbI$_5$ [9], Ag$_2$S [10] or Ag$_2$SO$_4$ [11] exhibit high ac-conductivity even at room temperature. The manufacturing of such glassy systems emerged from their industrial needs in many applications including electro-optical modulator for telecommunication [12], in electrochemistry including fibers for electrophysiology applications [13], photonic bandgap guidance of a solid core photonic crystal fiber (PCF) consisting of silver metaphosphate (AgPO$_3$) glass embedded in

a silica cladding for possible low-loss optical transmission along the PCF length for large range of frequencies and different environmental temperatures [14, 15].

In recent years, extensive research has been devoted to understand the basic mechanism underlying the improved electrical and dielectric properties of such glass mixtures [5]. The electrical conductivity of AgPO$_3$ network-like glasses is low $\sim 10^{-7}$ $(\Omega$ cm$)^{-1}$ [16], but when doped with solid electrolytes (e.g., AgI or Ag$_2$S) an increase in their electrical conductivity by a factor of 10^5 was observed at room temperature [16]. In other compositions like xAgI-$(1 − x)$AgPO$_3$, xNaI-$(1 − x)$AgPO$_3$ a noticeable increase in the conductivity has been achieved at different temperatures [5, 8, 17].

The purpose of the present work was to examine the effect of temperature and frequency on the dielectric behavior of AgPO$_3$ by employing ac-impedance spectroscopy measurements.

2 Sample perpetration

The glass (AgPO$_3$) was prepared by melting mixtures of appropriate amounts of NH$_4$H$_2$PO$_4$ and AgNO$_3$ in the powder form (purity > 99.8%) using the mole ratio technique [17, 18]. The mixture was heated in porcelain crucible at 300 °C for 2 hours to cease gas evolution. After that, the temperature was gradually increased to 600 °C and the sample was kept at this temperature for 2 h to complete the chemical reaction

---

✉ A. Shaheen
adel_shaheen@hu.edu.jo

1 Physics Department, Hashemite University, P.O. Box 150459, Zarqa 13115, Jordan

2 Department of Physics, University of Banha, Banha, Egypt

between the mixture components. The resulting melt was stirred continuously to ensure homogeneity. This procedure has proven to form a well-homogeneous network structure of the $AgPO_3$ lattice built form P–O chains held together by the Ag–O bridges [18]. Finally, the melt was poured on a steel plate to cool down to room temperature. The obtained bulk glass was polished carefully to give two perfect parallel surfaces to attach two excellent Ohmic electrodes on the glass surfaces. A silver paste (paint) was used for the glass surface coating, and the resulting coated glass was left at room temperature for the next day. The glass sample's density was measured using the suspension weight method based on the Archimedes principle using toluene as an immersion liquid. The determined value of the molar volume of $AgPO_3$ glass sample (41.3 cm^3/mol) is in excellent agreement with the reported value in [8].

3 Ac-impedance equipment

Ac-impedance measurements were carried out in the frequency range between 50 and 10^6 Hz and in the temperature range 30–110 °C using Solartron-1260 Impedance/Gain Phase Analyzer with 1296-dielectric interface. Two software packages, Z-60 and Z-View, were used to maximize the performance and data handling of the system. Measuring the amplitude and the phase shift of the resulting current allows one to calculate the real and imaginary components of the complex impedance. Finally, the real and imaginary components of dielectric constant, dielectric loss and ac-conductivity were determined and plotted as a function of frequency at different temperatures [19].

4 Data analysis

At a particular frequency, the complex ac-impedance Z^* and the complex dielectric constant ε^* can be expressed in terms of their real and imaginary parts as follows:

$$\left.\begin{array}{l} Z^* = Z' - jZ'' \\ \varepsilon^* = \varepsilon' - j\varepsilon'' \end{array}\right] \tag{1}$$

where Z', ε' are the real components and Z'', ε'' are the imaginary components and $j = \sqrt{-1}$. The relationship between the dielectric constants and ac-impedance can be written as:

$$\left.\begin{array}{l} \varepsilon' = Z' / \left(2\pi f C_o Z^2\right) \\ \varepsilon'' = Z'' / \left(2\pi f C_o Z^2\right) \end{array}\right] \tag{2}$$

where C_o is the geometrical capacitance.

The dc-conductivity was determined from the intersection points of the low- and high-frequency end of the semicircle on the Z'-axis using the following relation:

$$\sigma_{dc} = d / R_p A \tag{3}$$

where A is the cross-sectional area of the electrode, d is the thickness of the proposed capacitor and R_p is the bulk resistance determined from the intersections of the semicircle with the Z'-axis in the impedance complex plot.

The dc-conductivity is given by:

$$\sigma_{dc} = \sigma_a \exp\left(-E_a / k_B T\right) \tag{4}$$

where T is the absolute temperature, k_B is Boltzmann constant and E_a is the activation energy. A plot of ln (I) against $1/T$ yields a straight line whose slope is $-E_a / k_B$.

5 Results and discussion

The results in this paper were presented in terms of the real and imaginary components of the complex quantities Z^* and ε^* to study the effect of temperature on the dielectric properties of this chemical composition. These quantities were measured under ac-current with constant bias voltage of 0.2 mV at temperatures below the glass transition temperature of $AgPO_3$ ($T_g = 165$ °C) [18]. The measurements were carried out in the frequency range 50–1 MHz.

5.1 Ac-conductivity measurements

Figure 1 shows a plot of Z' and Z'' as a function of frequency for selected temperatures as indicated in the figure. The model-fitting of RC-circuit is also indicated in the panel. The real part of the complex impedance Z' for $T = 40$ °C was found to increase sharply with decreasing frequency in the range 50–10^3 Hz (see Fig. 1a). This pronounced behavior confirms the insulating character of the sample at this frequency range while it becomes frequency-independent thereafter. However, for higher temperatures which is exemplified by $T = 110$ °C, the real part Z' is frequency independent for $f < 200$ Hz, and then decreases steadily with frequency in the same manner as for the low temperature pinpointing to a capacitive behavior of the glass network [5, 18]. This behavior is common for the glassy network and can be attributed to the space charge-polarization effects within the interfacial glass surface at low frequency and the absence of such effect at high frequency [5]. Also, the variation of the imaginary part Z'' of the impendence with frequency is also indicated in Fig. 1b. For all temperatures studied here, the imaginary part Z'' exhibits a peak maximum which gradually shifted to higher frequency as the sample's temperature is increased. This phenomenon clearly indicates the electrical
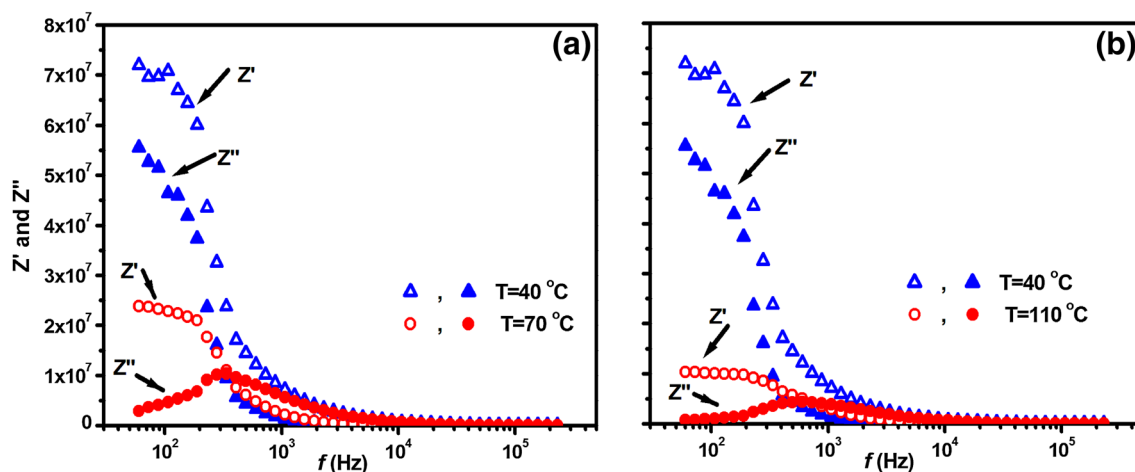
Fig. 1 The real (circles) and imaginary (triangles) parts of the impedance as a function of frequency at selected temperatures. The plot shows the behavior of Z′ and Z″ at low- (Fig. 1a) and high-temperature (Fig. 1b) regimes. Also, displaced in the panels is the model-fitting of the proposed RC-circuit

relaxation-temperature dependent within the glassy network [5, 20]. Figure 2 shows the Nyquist complex-plane impedance spectra obtained for AgPO₃ sample. The model-fitting of RC-circuit is also indicated in the panel. For each spectrum, the sample was heated to the indicated temperature and left there for more than 30 min to reach thermal equilibrium before conducting the measurement. The spectra profiles are indicative of a resistance–capacitance parallel electrical circuit. These electrical elements have been previously [5] introduced to reveal the hidden impedance properties of some dielectric materials. This modeling has successfully explained the behavior of many dielectric materials including crystalline and non-crystalline solids [6–8]. In addition, this model has been frequently used to explain the distribution of ionic charge carries in ionic conductors [7, 8]. The idea behind such a model was to enhance the fitting procedure for the obtained impedance spectra over the whole frequency range for any dielectric material [8]. Introducing the RC elements in the fitting process was essential to model the AgPO₃ glass complex impedance spectra as shown in Fig. 2a, b for the whole temperature range studied here. The equivalent RC-circuit that elucidates the dielectric behavior of the AgPO₃ glass is also obtained from the fitting program as shown in Fig. 2b. This simple RC-circuit could be applied for all temperatures investigated in the present study. This model can be easily understood as a frequency-dependent circuit. In the low-frequency regime, the contribution of the electrodes is more prominent than the glass sample itself, while in the high-frequency region, the glass-related capacitance (i.e., C) has less dominant effect in the electrical
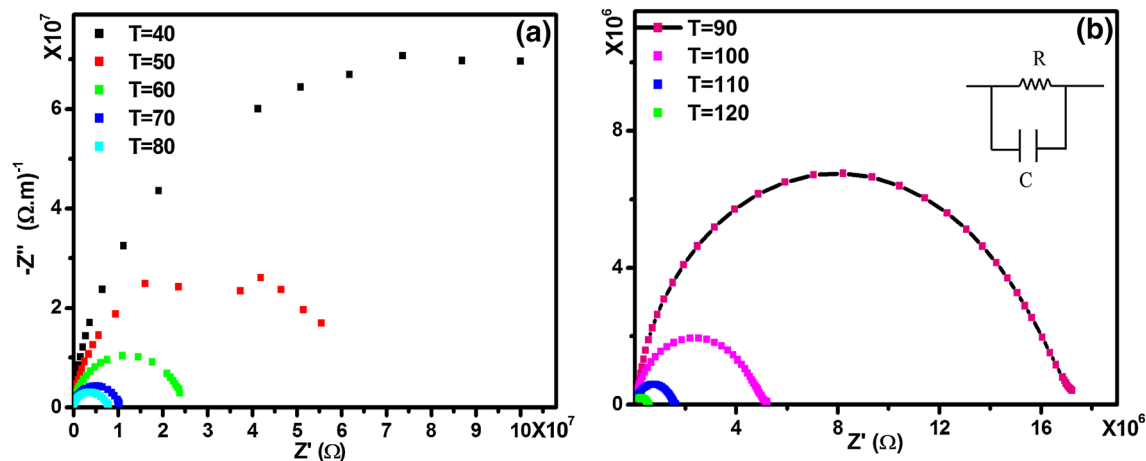

Fig. 2 The real part versus the imaginary part of the impedance complex plane. **a** For low and **b** for high temperatures. This plot features the transition from an open-circle to close-circle behavior of the Nyquist complex-plane spectra

properties than conduction resistance of the glass (R) with negligible effect due to electrode. It is worthwhile mentioning here that at low frequency, the intercept of the semicircle with the real axis showed no change with temperature, which indicates that the conductivity of the sample is frequency independent. This behavior can also be confirmed from the Z' versus f plot as seen in Fig. 1.

Along with these results, very recently, Rioux et al. [5] have reported on the opto-conductive behavior of AgI–AgPO$_3$–WO$_3$ glass fibers using ac-impedance spectroscopy from 1 Hz to 1 MHz. They studied the effects of temperature and tungsten oxide (WO$_3$) addition to the phosphate glassy network on the optical and electrical properties of such networking matrix. Their limited temperature effect measurements on the complex impedance of the studied glasses showed that the Nyquist profiles have a non-semicircle character but an open-like spectra complex curve indicative of a resistance–capacitance parallel circuit behavior. Reddy et al. [20] have investigated the ionic conductivity and dielectric relaxation properties of silver-based glasses mixed with phosphor–molybdate additives. Their study was conducted over the temperature range 25–80 °C from 10 Hz to 10 MHz. Their typical complex impedance plots have shown only one semicircle confirming the ionic conduction mechanism. Also, they have noted that the intersection point shifts toward lower Z' values with increasing temperature, which is a clear indicative of the dominant thermally activated dc-conductivity process.

5.2 Activation energy

Figure 3 shows the Arrhenius linear plot of $\ln(\sigma_{dc})$ against ($1/T$) which gives the dc-activation energy (E_a). The best linear fit of data gives an activation energy of $E_a = 0.47 \pm 0.02$ eV. The obtained value is in excellent agreement with other calculated values of Ag-based glass compounds [5–8, 20]. The typical values of E_a of glasses containing Ag$^+$ ions are found to lie between 0.39 and 0.54 eV. For example, Reddy et al. [20] have investigated the electric and dielectric properties of different types of silver ion-conducting glass (i.e., xAg$_2$SO$_4$–15Ag$_2$O–(90 − x) (90P$_2$O$_5$ − 10MoO$_3$); x is Ag molar fraction) systems over the temperature range 25–80 °C and frequencies between 10 Hz and 10 MHz. They found that there is a single activation energy barrier that drives the dc-conductivity of the network-forming glass matrix. Also, it has been reported that in binary glass systems such as AgPO$_3$–Ag$_2$SO$_4$, the dc-conductivity depends on the concentration of Ag$_2$SO$_4$ at temperatures well below the glass transition temperature [21]. The addition of modifiers to the glass network such as iodide and sodium ions and their subsequent effects on the conductivity has been investigated by Takahashi et al. [8]. They studied glass systems of the type NaI–AgPO$_3$ and concluded that the
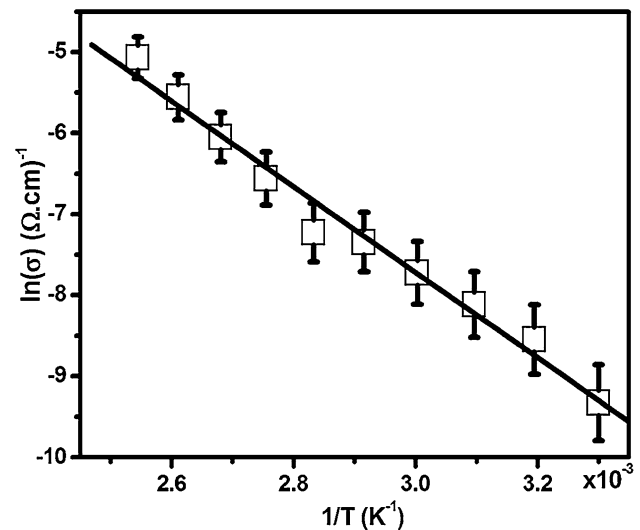

Fig. 3 The variation of the natural log of dc-conductivity with temperature inverse. The linear regression fitting of these data points was used to estimate the activation energy of the glass network to be $E_a = 0.47$ eV

crystals of AgI and NaPO$_3$ behave differently with respect to the glass transition temperature ($T_g = 250$ °C) of the whole glass matrix of (NaI)$_x$–(AgPO$_3$)$_{1-x}$. They found that the AgI crystal is precipitated at a certain composition beyond the glass-forming region of the matrix, while the crystallization of NaPO$_3$ appears near the T_g of the glass system.

This suggested that a preferential bonding between Ag and I ions rather than Na and I ions is governing the activation energy within NaPO$_3$ crystals [8]. Among the different glass samples studied in their report, the activation energy $E_a \in [0.38, 0.60]$ depends on the iodide content of the glass. Also Rioux et al. [5] have obtained an activation energy ranging from 0.15 to 0.4 eV depending on the tungsten oxide concentration in the glass network.

5.3 The frequency dependence of the total conductivity

Figure 4a illustrates the natural logarithmic plots of σ_{tot} (f) against frequency (f) in the range (50 Hz–5 MHz) at different temperatures. It is noticed that the total conductivity is fairly constant at the lower frequency range but it obeys a power relation at higher frequency for all temperatures used in this study. This two-regime variation of $\sigma_{tot}(f)$ with frequency can be expressed using the following relation [6]:

$$\sigma_{tot}(f) = \sigma_{dc} + \sigma'(f) \tag{5}$$

where σ_{dc} is the frequency-independent dc-conductivity (i.e., extrapolation of σ_{tot} to $f = 0$) and $\sigma'(f)$ is the ac-conductivity given by a power law of the form $\sigma'(f) = A\omega^s$, where $\omega = 2\pi f$. The constant A and the exponent s can be
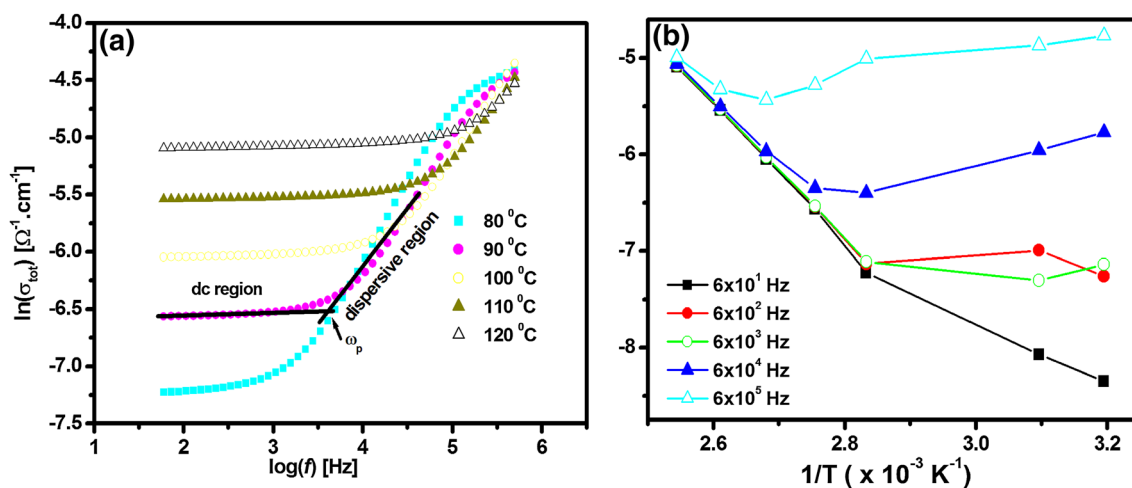
Fig. 4 The variation of the natural log of total conductivity as a function of **a** frequency at selected temperatures and **b** temperature inverse at selected frequencies. The plot reveals the crossover frequency (ω_p) along with the two distinct σ_{tot} characteristic behaviors

Table 1 The temperature, dc-conductivity $\omega_p = (\sigma/A)^{1/s}$ and hopping rate dependency along with the activation factor A and the exponent s of the AgPO$_3$ glass system

T (K)	ln (σ)	ω_p	A	s
353	−7.32	3.218	−7.56	−0.57
363	−6.60	3.780	−7.864	−0.60
373	−6.07	4.190	−10.510	−0.95
383	−5.56	4.705	−10.813	−0.97
393	−5.11	5.102	−9.013	−0.96

determined from the least square fitting procedure of $\sigma_{tot}(f)$ versus the frequency f. The general behavior of σ_{tot} as a function of frequency is a common feature with other related polymeric or glassy materials [5, 7, 9]. These two regimes are indicated in Fig. 4a by two lines describing the low- and high-frequency behavior. In addition, there is a crossover frequency ω_p after which the conductivity obeys the above-mentioned power law. Another important feature of ω_p is the monotone increase in its value as the sample's temperature increases. At this crossover frequency ω_p, the dielectric behavior of the glassy network changes from dc to dispersive region [5–7]. This common feature of such dielectric materials has been seen in many polymeric and glassy samples [16]. This dielectric behavior has been described in the work of Cutroni et al. [6] where the total conductivity reaches twice σ_{dc} at this critical frequency ω_p (defined as the ionic hopping rate) which is given by $\omega_p = \left(\sigma_{dc}/A\right)^{1/s}$. The values of ω_p are deduced at different temperatures for the glass system under investigation from Fig. 4a. The hopping rate ω_p values for all temperatures studied here are listed in Table 1. The values of ω_p were found to be thermally activated and obey the following Arrhenius relation:

$$\omega_p = \omega_o \exp\left(-E_\omega / k_B T\right) \quad (6)$$

where $E\omega$ is the activation energy concerning the variation of ω_p with temperature, and $\omega_p = \omega_o$ at $T = \infty$. The values of $E\omega$ and ω_o are deduced using the least squares fitting of the above relation leading to values of $E\omega = 0.88$ eV and $\ln(\omega_o) = 13.25$ rad/s. The observed increase of ω_p with increasing temperature can be explained as follows: the increase of ambient temperature leads to an increase in the dc-conductivity of the glass which competes with the influence of polarization.

5.4 The temperature dependence of total conductivity

Figure 4b shows the total conductivity σ_{tot} against ($1/T$) at selected frequencies (6×10^1, 6×10^2, 6×10^3, 6×10^4, 6×10^5 Hz). The total conductivity σ_{tot} was observed to be thermally activated over the entire temperature range studied here, where the variation of σ_{tot} with temperature can be divided into two regions. The observed anomaly in σ_{tot} appears at some frequencies as indicated in Fig. 4b. This behavior could be described by the following relation [6]:

$$T\sigma_{tot} = A \exp\left(-\Delta E_1 / k_B T\right) + B \exp\left(-\Delta E_2 / k_B T\right) \quad (7)$$

where A and B are temperature-independent constants and ΔE_1 and ΔE_2 are the low- and high-temperature activation energies of the glassy network. The observed behavior of σ_{tot} versus $1/T$ relation can be explained as follows: when the temperature was increased σ_{tot} increased because of structure relaxation and the Ag$^+$ ions attached to the non-bridging oxygen are released and become mobile leading to an increase in the mobile ion concentration. The activation energy values obtained from the fit of the conductivity at low

and high temperatures are 0.65 and 0.28 eV, respectively. A very low energy (about 0.28 eV) characterizing the relaxation process within the glassy network is in good agreement with the value obtained by Cutroni et al. for the same type of samples [6]. At higher temperatures, the obtained activation energy of 0.28 eV falls within the experimentally obtained results by different groups [20, 21]. This energy $0.26 < \Delta E < 0.28$ eV characterizes the second relaxation process in glassy systems.

Figure 5 shows the behavior of the imaginary part of the dielectric constant ($\ln(\varepsilon'')$) dependency on the natural log of the frequency (i.e., $\ln(f)$) in the range 50–10^6 Hz for different temperatures. It is noted that all the curves give a straight line up to 10^5 Hz. Linear regression fits give a slope value close to -1 (-0.97 and -0.57 for $T = 30$ and $T = 120$ °C, respectively). A strong evidence of dc-conduction is predominant in the studied sample over a wide range of temperatures. Above 10^5 Hz the dielectric constant behavior becomes non-linear which may be attributed to a more complex networking of the glassy materials at least at the surface of the samples (see supplementary materials provided online, Fig. S1) [18]. This observation along with the deviation of the slope from unity can be understood in terms of space charge polarization at low-frequency regime with no peak relaxation observed in the plot of ε'' versus f (see supplementary materials provided online, Fig. S2) [22].

6 Conclusions

In the present work, the dielectric properties of $AgPO_3$ glass network at different temperatures were analyzed based on electrical conductivity measurements. Two dielectric regimes have been found within the glassy network depending on the frequency range for all temperatures studied in this work. The total conductivity analysis reveals two relaxation processes with activation energies typical for such doped glass network. This study points to a promising application of this type of glassy system in the high-frequency and high-temperature fiber-sensing devices that require good electrical conductivity and stability during varying environmental conditions.

References

1. P.A. Mrozek, B.S. Kim, V.C. Holmberg, T.A. Taton, Nano Lett. **3**, 1665 (2003)
2. S. Ghose, K.A. Watson, D.M. Delozier, D.C. Workind, E.L. Siochi, J.W. Connell, Compos Part A **37**, 465 (2006)
3. C. Chan, G. Crawford, Y. Gao, R. Hurt, K. Jian, H. Li, B. Sheldon, M. Sousa, Y. Nancy, Carbon **43**, 2431 (2005)
4. S. Gorgustsa, V. Belanger-Garnier, B. Ung, J. Viens, B. Gosselin, S. LaRochelle, Y. Messaddew, Sensors **14**, 19260 (2014)
5. M. Rioux, Y. Ledemi, J. Viens, S. Morency, S.A. Ghaffari, Y. Messaddeq, RSC Adv **5**, 40236 (2015)
6. M. Cutroni, A. Mandanici, P. Mustarelli, C. Tomasi, M. Federico, J. Non-Cryst. Solids **307–310**, 963 (2002)
7. M. Mangion, G.P. Johari, Phys. Rev. B **36**, 8845 (1987)
8. H. Takahashi, H. Nakanii, T. Sakuma, Y. Onoda, Solid state Ionics **179**, 2137 (2008)
9. K. Funke, T. Kloidt, D. Wilmer, C.J. Carlile, Solid state Ionics **53–56**, 947 (1992)
10. A. Magistris, M. Villa, P. Mustarelli, M. Cutroni, Solid state Ionics **53–56**, 1232 (1992)
11. S. Scotti, M. Villa, M. Cutroni, A. Magistris, Solid state Ionics **53–56**, 1237 (1992)
12. I. Konidakis, G. Zito, S. Pissadakis, Opt. Lett. **37**, 2499 (2012)
13. M. Blais-Roberge, M. Rioux, Y. Ledemi, Y. Messaddeq, J. Non-Cryst. Solids **470**, 61 (2017)
14. D.P. Singh, K. Shahi, K.K. Kar, Solid State Ionics **287**, 89 (2016)
15. A. Mandanici, A. Raimondo, M. Federico, M. Cutroni, P. Mustarelli, C. Armellini, F. Rocca, J. Non-Cryst. Solids **401**, 254 (2014)
16. E. Kartini, Solid state Ionics **1**, 157 (2003)
17. A.C.M. Rodrigues, M.L.F. Nascimento, C.B. Bragatto, J-L. Souquet **135**, 234504 (2011)
18. C.B. Bragatto, D.R. Cassar, O. Peitt, J.-L. Souquet, A.C.M. Rodrigues, J. Non-Cryst. Solids **437**, 43 (2016)
19. S. Abdul-Jawad, A.S. Abu-Surrah, M. Maghrabi, Z. Khattari, Phys. B **406**, 2565 (2011)
20. C.N. Reddy, V.C.V. Gowda, Ionics **12**, 159 (2006)
21. J.P. Malugani, A. Wasniewski, M. Doreau, G.C.R. Robert. Acad. Sci. Paris **287**, C455 (1978)
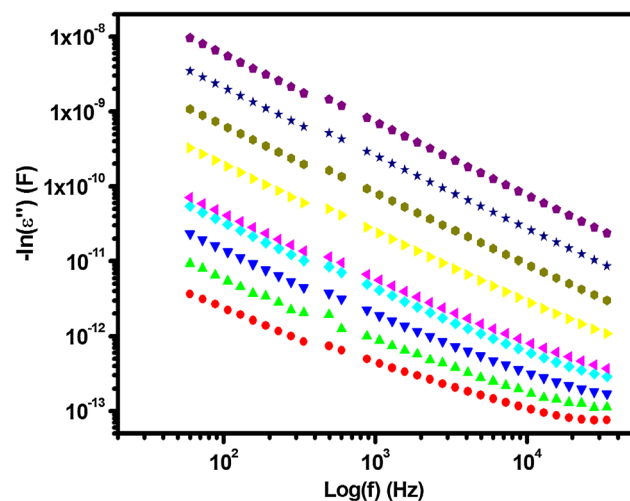22. P.B. Macedo, C.T. Moyniham, R. Bose, Phys. Chem. Glasses **13**, 171 (1972)

Fig. 5 The natural log of the dielectric loss as a function of frequency for all temperatures studied in this work. The figure shows the linear behavior of the dielectric loss up to $f = 3 \times 10^4$ Hz. The non-linear behavior after this frequency is presented in the supplementary information provided online in Fig. S2